American Mineralogist, Volume 63, pages 433–447, 1978

The spindle stage: a turning point for optical crystallography[1]

F. DONALD BLOSS

Department of Geological Sciences
Virginia Polytechnic Institute and State University
Blacksburg, Virginia 24060

Abstract

Spindle-stage methods combined with computer and statistical analysis of the resultant data promise a significant upgrading and expansion of the present optical data base for crystalline compounds. For example, the accurate crystal orientation achievable with a spindle stage, combined with a simple statistical treatment of double-variation data permit a crystal's principal indices to be determined to (*ca.*) 0.0005 for any visible wavelength and, with lesser accuracy, for near infrared and ultraviolet wavelengths.

DISPER, a subroutine recently added to the now modified Bloss and Riess (1973) program, provides quantitative measurements of dispersion for a biaxial crystal's five optic vectors—namely, the two optic axes plus X, Y, and Z—if the crystal's extinction data for up to four different wavelengths are measured. After the Bloss-Riess solution for each wavelength, DISPER calculates (1) the angular change in each vector, from one wavelength to another, and (2) the confidence level for rejecting the null hypothesis of non-dispersion. Extinction data for 433 and 666 nm wavelengths permitted rejection, at the 0.90 confidence level, of non-dispersion for all optic vectors *except the obtuse bisectrix* for an adularia from St. Gotthard, Switzerland, and for an albite from Tiburon, California. By contrast, an albite from Amelia Courthouse, Virginia, exhibited dispersion for the obtuse bisectrix as well. This dispersional difference between the two albites is puzzling. They agree in $2V_D$ by the Bloss-Riess method [77.1° (*esd* 0.3°), Tiburon; 76.9° (*esd* 0.3°), Amelia], and microprobe analyses indicate almost identical compositions. Indeed, by analogy to orthoclase and adularia, the slightly higher K_2O in the Amelia specimen would presumably *suppress* rather than foster dispersion of the optic normal. Does this subtle optical difference reflect different petrogenetic histories?

By determining the crystal's extinction positions with a photomultiplier or IR detector, $2V$ and the orientation of the five optic vectors become readily determinable (1) for non-visible wavelengths and/or (2) for the crystal at temperatures up to 1000°C or more. Such photometric measurements of extinction at 540 nm and 900 nm were made for a polished cylinder of Mijakejima anorthite *while* its temperature in degrees Celsius was held at 25, 200, 300, 350, 400, 500, 600, 700, 750, 800, 850—and during subsequent cooling—at 600, 500, 350, 200, and 25. Because extinctions were measured with the crystal cylinder in air, the Bloss-Riess solutions of the data for each temperature incorporated a small systematic error. Nevertheless, a plot of $2V$ versus temperature disclosed a well-defined minimum near 350°C, particularly for 900 nm. Highly magnified stereographic plots of positional change with temperature for each of the five optic vectors, particularly for 900 nm, usually showed sharp inflections near 350° during heating and during cooling. Thus, the gradual disappearance of the c reflections ($h + k$ even; l odd) that accompanies the continuous transition from 'primitive' to 'body-centered' anorthite as it is heated from 25°C to (*ca.*) 350°C is accompanied by measurable optical changes. These optical changes monitor the temperatures at which thermally-induced structural changes occur or achieve completion.

Introduction

The routine techniques of optical crystallography have improved little since Emmons (1928, p. 504) developed the double-variation method almost 50 years ago. In notable contrast, those of X-ray crystallography have been revolutionized by use of high-speed computers, statistical methods, and automation. Each year, as a result, more and more crystal structures have been solved or refined with ever-in-

[1] Presidential Address, Mineralogical Society of America. Delivered at the 58th Annual Meeting of the Society, November 8, 1977.

0003–004X/78/0506–0433$02.00

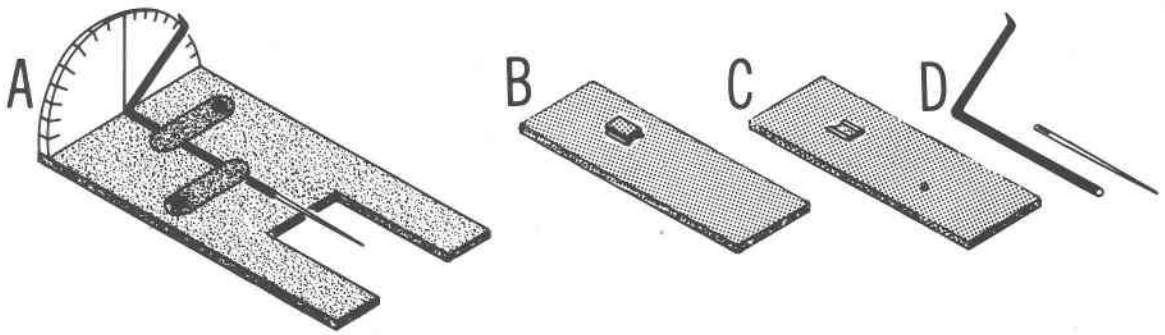

Fig. 1. A. The detent spindle stage (somewhat stylized). The knicks along the circular edge of the protractor scale are detents which cause the spindle to "click" into every 10° position. Ordinary glass slides (27 × 46 mm) slide snugly into the spindle stage's cut-out area or "dock." B. Typical glass slide with a small cover glass bridged across two tiny, square, brass rods. The immersion oil is inserted in the space between this cover glass and the glass slide. Thus, if this slide is inserted into the "dock" of the spindle stage, the grain on the spindle's tip will be between the cover glass and the glass slide (and will thus be immersed in the oil). C. Glass slide containing oil cell without a cover glass across the two rods cemented onto the slide. If the new oil is inserted into this open cell and the cell is inserted into the "dock," the grain on the spindle tip is rinsed with the new oil. Then slide (B), with its cell cleaned and filled with the new oil, can next be inserted into the dock so that the crystal's principal refractive indices can be measured relative to this new oil. D. The spindle, removed from its stage, consists of appropriately bent stainless steel tubing as used for hypodermic needles. Standard sewing needles fit into this tubing. These needles, with the grain cemented to their tips, are easily stored. From Bloss and Light (1973).

creasing precision by more and more researchers. Unfortunately, however, these many elegant structural determinations are frequently accompanied by optical data of insufficient accuracy or, worse yet, by none at all. For example, even the first descriptions of new minerals may cite principal refractive indices to ± 0.002 and only place $2V$ within a ten-degree range. The situation has led Mandarino (1977) to fear that the techniques of optical mineralogy are approaching extinction, and to ask, "Are people being trained in all the skills necessary to describe a new mineral?"

Mandarino's question seems well taken. Many mineralogists remain unaware of how easily and precisely the optical properties of a single crystal can be determined by use of a relatively inexpensive device, the spindle stage of Wilcox (1959) or its modification, the detent spindle stage of Bloss and Light (1973). This latter (Fig. 1) possesses a rigid protractor scale equipped with detents that cause the spindle tc "click" accurately into place at the spindle settings (S settings) 0°, 10°, ···, 180° on the protractor scale. It also incorporates two improvements suggested by Jones (1968): (1) a slide-away oil cell, which facilitates changing to another immersion oil; and (2) removable spindle tips so that a grain, cemented to a needle or glass fiber, can be removed from the spindle and either stored or transferred to an X-ray camera after its optical properties are measured. In common with any spindle stage, the detent stage retains the advantages over the universal stage enumerated by Wilcox (1959), namely: (1) *any* desired direction in the crystal may be rotated into the plane of the microscope stage so that all three principal indices, plus a value of $2V$ independent of that calculated from them, are directly determinable from the same grain; (2) no corrections need be made to the angular rotations, since the planar surfaces of the oil cell remain perpendicular to the microscope axis; (3) either orthoscopic or conoscopic illumination can be used; and (4) the methods are simple and the device is inexpensive.

The inherent simplicity and accuracy of just a few of the optical techniques developed for use in conjunction with the spindle stage will now be described, chiefly by means of examples. Their underlying theory and experimental details, as well as many additional techniques, are being omitted to save space and because full descriptions are available elsewhere (Bloss, in preparation).

Determining refractive indices and their dispersion

Variation of the wavelength of illumination to determine λ_1 and n_1, the wavelength and refractive index of match between a grain and the oil in which it is immersed, was first employed by Merwin and Larsen (1912) and later, combined with temperature variation, by Emmons (1928). The Emmons' method, originally called the *double-dispersion method* but later the *double-variation method,* produces grain-oil index matches at j different wavelengths and thus j data-pairs—$\lambda_1, n_1; \lambda_2, n_2; \cdots; \lambda_j, n_j$. Usually, mineralogists plot such data on a Hartmann dispersion net and, by visual estimation, draw the straight line of presumably best fit. Better reduction of the effect of

random errors was achieved by Bloss and Louisnathan (1974) and by Louisnathan *et al.* (1978), who fit accepted dispersion equations by least squares to such data. The latter authors used a particularly effective equation

$$y = a_0 + a_1 x \qquad \text{Eq. 1}$$

in which a_0 and a_1 are constants, y represents $(n_\lambda^2 - 1)^{-1}$, and x represents λ^{-2}. Equation 1 merely restates the single-term Sellmeier equation

$$n_\lambda^2 = 1 + \frac{A\lambda_\lambda^2}{\lambda_\lambda^2 - \lambda_0^2} \qquad \text{Eq. 2}$$

for which, if λ_λ represents visible wavelengths, then the constant λ_0 represents an absorption edge in the ultraviolet of strength proportional to the constant A.[2]

Since the indices were known for each of 222 Cargille oils at wavelengths 435.8, 486.1, 546.1, 589.3 and 656.3 nm, Louisnathan *et al.* (1978) transformed these data to the corresponding $(n_\lambda^2 - 1)^{-1}$ and λ^{-2} values in order to fit Equation 1 to them by simple linear regression. The coefficient of determination r^2 exceeded 0.999 for 217 oils and exceeded 0.997 for the remaining five.[3] The efficacy of Equation 1 was thereby checked and, equally important, the regression coefficients a_0 and a_1 thus evaluated for each Cargille oil permitted n_λ to be calculated for any visible wavelength λ_λ. This increased the utility of the Cargille oils since, once the wavelength of match between a grain and oil was established, the corresponding index of match could be calculated from Equation 1.

The refractive indices at various visible wavelengths were measured by Louisnathan *et al.* (1978) for two homogeneous optical glasses by immersing grains thereof in standard Cargille oils and varying wavelength until the Becke line disappeared or the oblique shadows reversed. A Leitz-Schott wedge interference filter proved adequate as a monochromator (Fig. 2), as did a set of interference filters with peak wavelengths at 20 nm intervals. The temperature of the oil was measured by a mercury thermometer (calibrated from 20° to 30°C in tenths) in contact with the oil cell's coverglass. Later, to reduce the number of oil mounts needed, an electric heating wire plus a thermocouple were installed in the oil cell. For each glass, Equation 1 was fitted to the resultant $(n_\lambda^2 - 1)^{-1}$ and λ^{-2} data. The coefficient of determination r^2 exceeded 0.995 in both cases and the resultant a_0 and a_1 values, when substituted into Equation 1, permitted the glass's refractive indices to be calculated to within 0.0003 for wavelengths between 365 and 706.5 nm and to within 0.0016 for the lengthy extrapolation to infrared wavelength 1083 nm (Louisnathan *et al.*, 1978, Table 4).

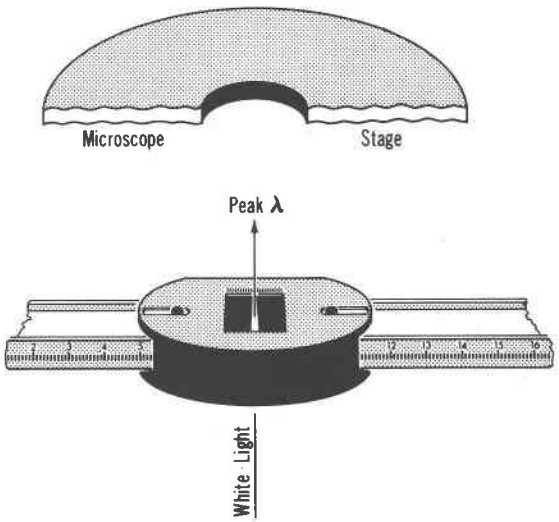

Fig. 2. A Leitz-Schott wedge interference filter inserted into its substage holder (from Bloss, in press).

Possible systematic errors

If indices to within 0.0003 at 25°C are being sought, oil-mount temperatures differing from 25°C by more than 10° should be avoided when using the double-variation technique, at least for some minerals. To illustrate, a temperature increase from 25° to 35°C will decrease γ_D by 0.00037 for anglesite but by only 0.00007 for anhydrite (Kolb, 1911).

Another possible systematic error, usually so small as to be obscured by the random errors, may result if the human eye is used to observe Becke line disappearances or oblique-shadow reversal during the double-variation method. As discussed by Louisnathan *et al.* (1978), the error results from the human eye having peak sensitivity near 555 nm under conditions of normal brightness (photopic vision). Its consequence is that the empirically-determined dis-

[2] Substances transparent within the visible region generally absorb a broad range of ultraviolet wavelengths centered at a wavelength here designated λ_0. For such substances, which are the ones dealt with in optical crystallography, Equations 1 and 2 hold well in the visible region (normal dispersion) but fail in the ultraviolet to the extent λ_λ approaches λ_0 in value. For substances with strong absorption (λ_0) in the visible region, Equations 1 and 2 will then fail in the visible region, such substances then exhibiting *anomalous dispersion.* See Jenkins and White (1976, p.482 *et seq.*)

[3] In other words, over 99% of the variation in y can be explained by a linear dependence upon x.

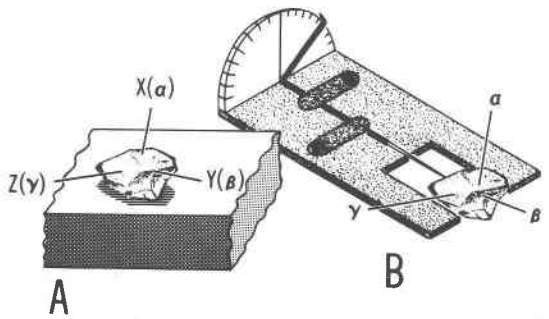

Fig. 3. For a biaxial crystal, vastly exaggerated in size relative to the spindle stage, the positions of its three principal vibration axes—X, Y, and Z—are as shown. Note that for each there exists a spindle axis setting S that will orient this principal axis parallel to the plane of the stage. Consequently, the principal indices α, β, and γ can be each measured from this one grain.

persion curve may slope a bit more steeply than the true dispersion curve and intersect the true curve near 555 nm.

Determining $2V$ and indicatrix orientation

In order to measure the principal refractive indices α, β, and γ for a biaxial crystal, one must orient the corresponding axes X, Y, and Z of the optical indicatrix parallel to the microscope stage and to the polarizer's privileged direction. Such orientation is quickly and accurately accomplished with a spindle stage. Instead of being frustrated by grains resting in random orientations on the glass slide, the operator can rotate the crystal around the spindle axis until X, Y, or Z, as desired, lies in the plane of the microscope stage (Fig. 3). The microscope stage can then be rotated about the microscope axis M to the setting M_S that orients this axis parallel to the polarizer so that the corresponding principal refractive index can be measured.

The S and M_S settings required to orient each axis of the indicatrix parallel to the microscope stage and to the polarizer are determinable either conoscopically or orthoscopically. The conoscopic methods are rapid and serve to educate the student in the interpretation of interference figures. The orthoscopic methods apply to grains too small to yield interference figures, and also serve as non-destructive techniques for determining $2V$ and the orientation of the indicatrix for anisotropic inclusions in transparent isotropic crystals such as diamond. Moreover, compiling the orthoscopic extinction data for a crystal on a spindle is exceedingly simple. One only needs to set the spindle-stage arm to read successively 0°, 10°, ···, 170° on its protractor scale and for each such S setting to rotate the microscope stage to the setting (M_S) that causes the crystal to become extinct between crossed polars. Generally, each M_S value should represent the average of three or four careful determinations. The resultant orthoscopic data may be solved by stereographic projection or by BRR, the computer program of Bloss and Riess (1973) as modified by Rohrer. Both methods, as well as conoscopic techniques, are discussed elsewhere in detail (Bloss, in press).

Example

The output of the computer program is here given for extinction measurements made at 589 nm on an anorthite from Mijakejima, Japan (Fig. 4). This output thus discloses the value of $2V$ for 589 nm and the S, M_S settings needed to orient the crystal so that α, β, and γ for 589 nm can be each measured relative to the oil. With the orientation problem solved so neatly, the refractive indices of anisotropic crystals are as easy to measure as those of isotropic crystals. For most triclinic crystals the dispersion of the indicatrix axes is relatively modest, so that the S,M_S settings used to measure the grain's principal indices for wavelength 589 nm do not introduce significant error if also used to measure these principal indices for other visible wavelengths, say 450 nm or 650 nm. Alternatively, the crystal's extinctions could be determined at wavelengths 450 nm and also at 650 nm, for example, to determine the precise S,M_S settings needed to orient the crystal for measuring its principal refractive indices for wavelengths 450 and 650 nm.

The Mijakejima anorthite was selected for study since its refractive indices had been previously measured with great care by Leisen (1934), who used the method of minimum deviation upon prisms cut and polished from large clear crystals. For a spindle-stage-mounted crystal of Mijakejima anorthite for which the needed orientations had been previously determined (*cf.* Fig. 4), 28 matches at different wavelengths were obtained for α, 34 for β, and 35 for γ, using various Cargille oils. To the resultant data, corrected to 25°C and transformed to $(n_i^2 - 1)^{-1}$ and γ_i^{-2}, Equation 1 was fitted to obtain values of a_0 and a_1 which permitted the refractive indices to be estimated for any desired wavelength. When the principal refractive indices were calculated for the same wavelengths as had been used by Leisen, the agreement was within 0.0004 (Table 1) except for γ at 687 nm. For γ, the Leisen value of 1.5821 appears suspect, since (1) it yields a $2V$ value that is at variance with those calculated from the indices or from ex-

tinction data, and (2) in conjunction with his values for wavelengths 486 and 589.3, it does not yield a linear relationship between $(n_1^2 - 1)^{-1}$ and γ_1^{-2} unless this 1.5821 value is increased to about 1.5835. Aside from this, the agreement is remarkable, considering that the writer's crystals were not necessarily from the same outcrop as Leisen's. Technologically, the spindle-stage method was much more simple than the minimum-deviation method used by Leisen. A Schott-Leitz wedge interference filter (Fig. 2) had served as a very simple monochromator. A wire heating unit and a thermocouple to monitor temperature were, however, added to the spindle stage cell so as to reduce the number of oil mounts needed.

Dispersion of directions

The dispersion of the five basic optic directions—namely, the two optic axes (A1 and A2), their two bisectrices (AB and OB), and the optic normal (ON)—can be measured quantitatively if the crystal's extinction positions for spindle settings $S = 0°$, $10° \cdots$, $170°$ are determined for several different wavelengths of illumination. In such case, if data sets for several, preferably widely different, wavelengths are submitted to BRR, the program will calculate for each wavelength the cartesian coordinates for each of the five basic optic directions. These coordinates refer to the cartesian axes agreed on for microscopy by the German microscope manufacturers, that is, $+x$ is due east, $+y$ due north, and $+z$ represents the direction that light travels along the microscope axis. After solutions are obtained for each individual wavelength (up to four), a subroutine called DISPER can now be invoked to calculate (1) the angular changes in the five directions from one wavelength to the next and (2) the confidence level, based on a chi-squared value,

Table 1. Comparison of the refractive indices measured for the Mijakejima anorthite by Louisnathan *et al.* (1978) using spindle-stage methods with those measured by Leisen (1934) using minimum deviation.

λ	486 nm		589.3 nm		687 nm	
	This	Leisen	This	Leisen	This	Leisen
α	1.5811	1.5808	1.5738	1.5741	1.5698	1.5700
β	1.5886	1.5886	1.5818	1.5821	1.5781	1.5777
γ	1.5936	1.5940	1.5871	1.5874	1.5835	1.5821*
$2V_{calc}$	101.9°	100.8°	102.1°	102.1°	102.6°	106.1°
2V from extinction:**						
	$2V_{550}$ = 101.4°		$2V_{589}$ = 102.3°		$2V_{660}$ = 102.7°	

*Probably in error.
**Determined with the method of Bloss and Riess (1973) as modified by Roberts (1975).

MIJAKEJIMA ANORTHITE, 589 NM

MR = 359.23

S	MS	ES	CES	ES-CES
0.0	46.78	47.55	47.55	-0.00
10.0	44.75	45.52	45.51	0.01
20.0	39.60	40.37	40.31	0.06
30.0	29.07	29.84	29.80	0.04
40.0	13.35	14.12	14.28	-0.16
50.0	360.08	0.85	0.84	0.01
60.0	351.72	82.49	82.41	0.08
70.0	346.08	76.85	76.89	-0.04
80.0	341.80	72.57	72.62	-0.05
90.0	337.97	68.74	68.79	-0.05
100.0	334.50	65.27	64.97	0.30
110.0	330.25	61.02	61.02	-0.00
120.0	325.85	56.62	56.94	-0.32
130.0	322.07	52.84	52.90	-0.06
140.0	318.53	49.30	49.15	0.15
150.0	315.30	46.07	45.97	0.10
160.0	312.90	43.67	43.63	0.04
170.0	311.50	42.27	42.36	-0.09

$2V_\gamma$ = 102.29 (esd 0.19)

COMPUTED DIRECTION COSINES

	X	Y	Z
OA1	-0.2941(14)	-0.5725(15)	0.7653(11)
OA2	0.7787(12)	0.4921(17)	0.3892(18)
AB	-0.6888(06)	-0.6835(07)	0.2415(08)
OB	0.3863(14)	-0.0641(23)	0.9202(07)
ON	-0.6135(13)	0.7271(07)	0.3082(24)

COMPUTED SPINDLE STAGE COORD. (Degrees)

	S	E	LOWER POL'R	
			E-W	N-S
OA1	126.8(1)	107.1(1)		
OA2	38.3(2)	38.9(1)		
AB	160.5(1)	133.54(1)	132.8	42.8
OB	94.0(1)	67.3(1)	66.5	336.5
ON	23.0(2)	127.8(1)	127.1	37.1

Fig. 4. Reorganization of the output after BRR solved extinction measurements made at wavelength 589 nm for an anorthite crystal from Mijakejima, Japan. The dashed rectangle has been added to enclose the input data—that is, the spindle setting *S* plus the microscope setting *MS* that brought the crystal to extinction. *ES* is the angle between each extinction direction and the spindle axis. BRR obtains this by subtracting from *MS* the value of *MR*, which is the microscope stage setting (reference azimuth) that oriented the spindle axis exactly east-west. *ES* is confined to the range 0° to 90° (by successive addition or subtraction of 90°, if needed). *CES* represents the values of *ES* computed from the two solved positions for the optic axes.

For each of the five optic vectors, BRR prints their computed direction cosines, spindle-stage coordinates, and their associated estimated standard deviations. Parenthesized figures indicate the estimated standard deviation (*esd*) in terms of the least units cited for the value. Thus, −0.2941 (14) indicates an *esd* of 0.0014 for the coordinate −0.2941 of OA1 relative to the *x* cartesian axis. The computed spindle-stage coordinates for AB, for example, indicate that, to measure the refractive index corresponding to the acute bisectrix (AB), the spindle's arm should be set at (*ca.*) 160.5° and the microscope stage reading should be set at 132.8° for a microscope with an E–W polarizer or at 42.8° for one with a N–S polarizer.

Table 2. Sample calculation* of χ^2 for the change in cartesian coordinates of an optic axis from wavelength 433 nm to wavelength 666 nm (from Bloss, in preparation).

	x (esd)	y (esd)	z (esd)
λ=1	0.229834(0.001977)	0.971975(0.000483)	0.049404(0.002554)
λ=4	0.240436(0.002206)	0.968934(0.000572)	0.057941(0.002885)
DIFF	0.010602	0.003041	0.008537
SEDIFF	(0.00344361)	(0.0009348)	(0.00454811)
$\left(\frac{\text{DIFF}}{\text{SEDIFF}}\right)^2$	9.479	10.583	3.523
χ^2 =	9.479 + 10.583 + 3.523 = 23.59		

*Explanation: The values in parentheses behind each coordinate in this table represent the estimated standard deviation of that coordinate. Let $\underline{esd}_i$ and $\underline{esd}_j$ represent those for $\underline{x}_i$ and $\underline{x}_j$, the coordinates relative to axis $\underline{x}$ of a given optic direction as determined for two different wavelengths, $\underline{i}$ and $\underline{j}$. DIFF represents the difference $|\underline{x}_i - \underline{x}_j|$. Ordinarily the standard error of this difference (SEDIFF) would be calculated as

$$\sqrt{(\underline{esd}_i)^2 + (\underline{esd}_j)^2}$$

However, as discussed in the text, a degree of uncertainty exists in calculating esd values. To guard against $\underline{esd}_i$ and $\underline{esd}_j$ being in error by being too low, which might result in an unwarranted rejection of the null hypothesis of non-dispersion, the absolute value of their difference $|\underline{esd}_i - \underline{esd}_j|$ is added to whichever is larger, $\underline{esd}_i$ or $\underline{esd}_j$. The resultant value, multiplied by 2, is then taken to be SEDIFF.

at which one can reject the null hypothesis that the direction remains fixed as wavelength is varied.

Examples

Extinction data for an albite from Tiburon, California were determined using interference filters with peak wavelengths at 433, 500, 600, and 666 nm. The computer's solutions then yielded, for each wavelength, the cartesian coordinates and their estimated standard deviations (*esd*) for unit vectors along each of the five optic directions. For brevity, the resultant coordinates and *esd*'s are given in Table 2 only for optic axis A1 at wavelengths 433 and 666 nm. The computer program calculates the difference in these coordinates for each wavelength (DIFF, Table 2), and the standard error of each such difference (SEDIFF, Table 2). Ordinarily the standard error of this difference would be calculated as

$$\text{SEDIFF} = \sqrt{(esd_{433})^2 + (esd_{666})^2} \qquad \text{Eq. 3}$$

However, any experimental errors which cause esd_{433} and/or esd_{666} to be calculated too low would contribute toward incorrectly large chi-squared values and hence to an unwarranted rejection of the null hypothesis of non-dispersion (of A1 in this case). As discussed in the footnote to Table 2, the program partly guards against this by increasing each of the two *esd* values until each exceeds the larger by their difference Δ. For example, assuming esd_{666} exceeds esd_{433} by an amount Δ, then Equation 3 becomes

$$\text{SEDIFF} = \sqrt{2(esd_{666} + \Delta)^2} = \sqrt{2}\,(esd_{666} + \Delta).$$

Using this upward-adjusted value of SEDIFF, the computer calculates (DIFF/SEDIFF)^2 for the x, y, and z coordinates of A1 and sums these values (Table 2) to obtain χ^2 for A1. When χ^2 has two degrees of freedom, the corresponding tail-area probability P can be calculated since

$$P = e^{-1/2\chi^2} \qquad \text{Eq. 4}$$

Consequently, the null hypothesis of non-dispersion may be rejected at a confidence level equal to $(1 - P)$. Thus a χ^2 value of 23.59 permits the null hypothesis of non-dispersion to be rejected at the 99.999 level.

Unfortunately, an optic direction's angles to the three cartesian axes x, y, and z govern, in part, the *esd* values calculated by BRR for its coordinates relative to these axes. For example, *esd* values become small as a coordinate approaches 1.0 in value—that is, as the optic direction becomes parallel to a cartesian axis. To guard against this effect, subroutine DISPER performs the χ^2 calculations summarized in Table 2 for each of the five basic optic vectors *as the y and z cartesian axes* but not the input data *are rotated about x by* (1) 0°, (2) 10° ··· (8) 70°, and (9) 80° *relative to these five vectors.*[4] For each vector, following the harmonic-mean rule of thumb of Good (1958, p. 799), the equivalent tail-area probability of its nine χ^2 values is computed by DISPER where now

$$P = 9 \Big/ \sum_{i=1}^{9} e^{1/2\chi_i^2} \qquad \text{Eq. 5}$$

The value of P obtained from Equation 5 is then used to calculate $(1 - P)$, the confidence level at which the null hypothesis (of no dispersion) may be rejected for the optic direction. Unless $(1 - P)$ equals or exceeds 0.9, the writer does not reject the null hypothesis.

The computer output from DISPER for the Tiburon albite (Table 3) contains some discrepancies, mostly because some wavelength changes—for example 433 to 500 nm—did not produce a sufficiently large change in the positions of the optic directions to permit rejection of the null hypothesis. Between the two extreme wavelengths, 433 and 666, however, one would expect the largest changes and thus the most

[4] Although such rotation does not change the angles of the five optic vectors relative to the x (spindle) axis, this will not be serious if the crystal was mounted on the spindle so as to pass the "40° test" of Wright (1966). This in itself will insure non-parallelism between cartesian axis x and optic directions X or Z.

reliable results. The 433–666 comparison permits rejection of the null hypothesis for all but the obtuse bisectrix. This dispersion thus resembles the *parallel* or *horizontal dispersion* of those monoclinic crystals whose obtuse bisectrix coincides with a 2- or $\bar{2}$-fold axis and hence does not undergo dispersion. The results thus confirm those cited by Winchell and Winchell (1951, p. 275), who describe the dispersion in albite as "horizontal, very weak."

For an adularia from St. Gotthard, two sets of extinction data had been measured by Dr. Michael W. Phillips for wavelengths 433, 566, and 666 nm, the data sets being those reproduced by Bloss and Riess (1973, Table 1). Their analysis by DISPER showed that, between wavelengths 433 and 666 nm, the null hypothesis of non-dispersion could be rejected at the 0.90 confidence level for the acute bisectrix (Table 4), for the optic normal (for set 1), but not for the obtuse bisectrix. Dispersion of just *one* of the three principal vibrations—AB, OB, or ON—is physically impossible and must be accompanied by dispersion of at least one other of the trio. Consequently, the dispersion unequivocally demonstrated for the acute bisectrix can be presumed to be accompanied by significant dispersion of the optic normal [for which even the lowest confidence level (Table 4) much exceeds those for the obtuse bisectrix]. Such dispersion again approximates the horizontal dispersion of monoclinic crystals and confirms the dispersion of adularia to be "horizontal, distinct" as reported by Winchell and Winchell (1951, p. 275). Note that the angular changes for the optic directions between wavelengths 433 and 666 nm, except for the obtuse bisectrix, are greater for the St. Gotthard adularia than for the Tiburon albite, this causing its dispersion to be more distinct.

Dispersion analyses for an albite from Amelia Courthouse, Virginia (Table 4) indicate triclinic dispersion—that is, dispersion of the optic normal and *both* bisectrices. This difference in dispersion relative to the Tiburon albite is puzzling. For each, $2V_D$, as determined by the Bloss-Riess technique, was essentially the same—77.1° (*esd* 0.3°) Tiburon versus 76.9° (*esd* 0.3°) Amelia. By microprobe analysis (P. H. Ribbe, personal communication) both seemed almost equally pure, with Fe content near zero and An content about one mole percent, except that the orthoclase content was 1 percent for the Amelia versus (*ca.*) 0 percent for the Tiburon specimen. By analogy to orthoclase and adularia, the slightly higher orthoclase content for the Amelia specimen would have been expected to *suppress* rather than foster the observed dispersion of its obtuse bisectrix. The question of this subtle optical difference between the two albites is thus moot. Does it arise because of different petrogenetic histories?

Combined optical and X-ray studies

To perform X-ray and optical measurements on the same crystal, a spindle stage that accommodates an X-ray goniometer head is best used. In such case, one can: (1) transfer the goniometer head between microscope and X-ray camera without loss of crystal orientation; and (2) from the Bloss-Riess optical solution, determine the settings of the goniometer head's arcs that will orient a non-triclinic crystal with

Table 3. Dispersion of the five optic vectors for a crystal of Tiburon albite as calculated by DISPER from visual extinction measurements made by E. Wolfe for wavelengths 433, 500, 600, and 666 nm.*

WAVELENGTHS (NM)		OPTIC AXIS 1	OPTIC AXIS 2	AB	OB	ON
433	500	0.14 (0.213)?	0.32 (0.636)	0.11 (0.507)?	0.36 (0.541)	0.37 (0.632)?
433	600	0.63 (0.998)	0.21 (0.256)	0.34 (0.996)	0.43 (0.735)	0.54 (0.984)
433	666	0.80 (1.000)	0.83 (0.992)	0.53 (1.000)	0.04 (0.010)	0.53 (0.995)
500	600	0.74 (1.000)	0.34 (0.742)	0.24 (0.931)	0.79 (0.985)?	0.81 (0.999)
500	666	0.86 (1.000)	0.65 (0.945)	0.42 (1.000)	0.31 (0.507)	0.52 (0.997)
600	666	0.38 (0.933)	0.67 (0.980)	0.21 (0.973)	0.48 (0.756)	0.51 (0.874)?

* The values not in parentheses represent the angle between the positions of the optic direction for the two wavelengths on the left and the value in parentheses represents the confidence level at which the null hypothesis (of non-dispersion) can be rejected for this optic direction. Thus under OPTIC AXIS 1, the values 0.63 (0.998) indicate that an angle of 0.63 was calculated between its positions at 433 and 600 nm and that the null hypothesis can be rejected at the 0.998 level. A question mark indicates values with confidence levels that may be out of kilter with the other confidence levels in this column.

Table 4. Comparison of DISPER's analysis of directional dispersion for two albites and an adularia between wavelengths 433 nm and 666 nm.

OA1	OA2	AB	OB	ON
TIBURON ALBITE (horizontal dispersion)				
0.80° (1.000)	0.83° (0.992)	0.53° (1.000)	0.04° (0.010)	0.53° (0.995)
AMELIA ALBITE (triclinic dispersion) Grain 1, Trials 1 and 2				
0.28° (0.516)	0.93° (0.980)	0.41° (1.000)	0.69° (0.998)	0.77° (1.000)
0.25° (0.845)	0.88° (1.000)	0.47° (1.000)	0.75° (1.000)	0.88° (1.000)
Grain 2 (Before heating)				
0.67° (0.998)	0.92° (0.999)	0.69° (1.000)	0.30° (0.960)	0.66° (1.000)
Grain 2, after heating at 200°C for 6 days				
0.70° (1.000)	1.06° (1.000)	0.47° (1.000)	0.21° (0.996)	0.42° (1.000)
ADULARIA, ST. GOTTHARD (horizontal dispersion)				
1.26° (0.982)	0.78° (0.813)	1.13° (0.998)	0.45° (0.514)	1.083 (0.912)
1.46° (0.999)	1.42° (1.000)	0.86° (0.999)	0.06° (0.011)	0.862 (0.872)

a direct axis parallel and/or a reciprocal axis perpendicular to the X-ray beam. Capability (1) will permit quantitative measurements of optical orientation relative to crystallographic axes. Capability (2) will reduce the number of X-ray exposures needed to orient a non-triclinic crystal. The techniques and calculations involved have been described at length by Bloss (in press), and hence need not be discussed here.

Studies beyond the visible and at elevated temperatures

A major advantage of orthoscopic relative to conoscopic spindle-stage techniques lies in the option of substituting a photomultiplier tube or infrared detector for the human eye when measuring crystal extinction. This extends the frontiers of optical crystallography beyond the relatively narrow visible spectrum (*ca.* 400–700 nm) and permits $2V$ and optic orientation to be determined by BRR for non-visible wavelengths as well. An immediate dividend will be increased reliability in DISPER's assessment of directional dispersion in biaxial crystals, because results for more widely separated wavelengths—say, 300, 600 and 900 nm—can then be compared. Even more exciting is the ability of orthoscopic techniques to determine $2V$ and optic orientation *while* the crystal is heated to temperatures up to 1000°C or more. This will permit the temperatures of many thermally-induced phase transitions to be determined with great sensitivity. Prior to demonstrating this for the Mijakejima anorthite, however, the equipment and procedures involved need to be briefly described and discussed.

Control and range of wavelength

From the spectrum of a xenon arc lamp (XBO-150), the desired visible wavelength bands were isolated by an interference filter with peak transmission at 540 nm and by a Schott (VERIL IB 200) variable IR filter set to transmit a peak wavelength at 900 nm. An attempt to isolate a UV band was unsuccessful because long wavelengths "leaked through" the UV interference filter used. A photomultiplier tube (RCA spectral response 119), in a light-tight case atop the ocular of a Leitz Ortholux microscope, monitored the intensity of the light transmitted by the upper polar as the crystal was being rotated to an extinction position. With this impromptu set-up, crystal extinctions were measurable for wavelengths between (*ca.*) 370 nm, the shortest transmitted by glass of the microscope, and (*ca.*) 900 nm, the longest detectible by the photomultiplier tube at hand. However, with some minor modifications—namely, use of quartz optics, special UV cemented calcite polarizers, and a photomultiplier tube with a wider sensitivity range, possibly RCA 101—investigations in the 300 to 1070 nm

range would become possible. Indeed, with a suitable IR detector and source, the long wavelength range could be greatly extended to permit Bloss-Riess solutions for crystals that are opaque to visible wavelengths but not to infrared.

Sample shape and preparation

At elevated temperatures for which the immersion oils decompose or vaporize, a crystal's extinction positions must be measured while it is in air ("dry"). To permit this, the crystal must be shaped and polished into a sphere or, better, into a cylinder[5] coaxial with the spindle so that light will pass through it for all settings (*S*) of the spindle, even though the crystal is not immersed in an oil. Orthoscopic spindle-stage techniques are subject to error if the wave-normal of the light, during passage through the crystal, deviates from parallelism with the axis of the microscope. In this event the crystal's extinction directions for a given spindle setting will not be exactly 90° apart. The absence of an immersion oil thus accentuates (1) the lens-like refraction of light by a crystal cylinder as well as (2) any irregularities in refraction caused by deviations from a truly cylindrical shape. The effect of such refraction errors can be assessed if extinctions are measured for the crystal cylinder in air and also in a closely-matching oil. The difference between the Bloss-Riess results for the two sets of data will indicate the amount of error from refraction by the dry cylinder.

The furnace and its calibration

A furnace to accommodate the heater devised by Brown *et al.* (1973) was fashioned from Macor, a machinable ceramic manufactured by the Corning Glass Company (Fig. 5). A polished cylinder of Mijakejima anorthite, affixed to a quartz-glass capillary tube with the high-temperature ZrO_2 cement described by Brown *et al.* (1973), was held on the goniometer head of a Supper spindle stage. The goniometer head's arcs had been carefully adjusted so that the crystal cylinder was coaxial with the spindle's axis of rotation. This insured that the crystal cylinder, after its insertion into the furnace's chamber via the 1/8″ entry hole, would turn freely as the spindle was rotated on its (*S*) axis.

A quartz glass slide, clamped onto the base of the Macor furnace, insured that, if the crystal dropped off the capillary tube, it would not be lost in the condenser of the microscope. Two sheets of heat-resistant Kapton film, separated by an air space and held in a metal ring, were placed atop the furnace to prevent upward heat loss and consequent overheating of the objective or filters. A 1/8″ hole in each sheet permitted the light beam, after passage through the crystal cylinder, to emerge from the furnace without

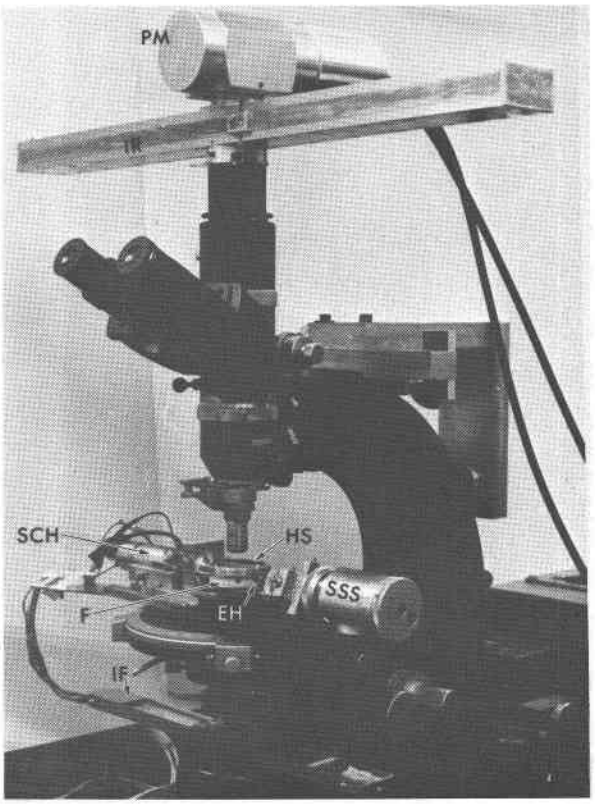

Fig. 5. Experimental arrangement during the heating experiments. The substage Leitz-Schott interference filter (*IF*) was removed from its holder. A cylinder of anorthite was mounted on the goniometer head of a Supper spindle stage (*SSS*) and the arcs of this head were adjusted until the cylinder and spindle stage were coaxial. The hollow Macor furnace (*F*) enclosed the heating element of the single crystal heater (*SCH*) devised by Brown *et al.* (1973). By sliding this heater and enclosing furnace along a track, the crystal was caused to enter the horizontal 1/8″ diameter entry hole (*EH*) in the furnace. A vertical hole in the furnace then permitted light to pass through the crystal cylinder and enter the objective. The Kapton heat shields (*HS*) had holes in them so that they did not intercept the light. Nevertheless, they did effectively prevent the upward escape of heat. A Schott-Leitz interference filter similar to *IF*, but for near infrared wavelengths, was enclosed in the light-tight holder (*IR*). A photomultiplier tube *PM* monitored the intensity of the light passing through the crystal between crossed nicols. For extinction measurements at 540 nm, an interference filter with peak at 540 nm was placed above *HS*, the heat shield, and the *IR* filter was adjusted in its light-tight box until it did not intercept the light.

[5] Thus far the fabrication of polished crystal cylinders has, for the writer, proven to be more an art than a science. The problems vary markedly with cleavage and hardness.

Table 5. Hours held at temperature before performing the extinction measurements on the anorthite cylinder during the heating cycle.

	200°	300°	350°	400°	500°	600°	700°	750°	800°	850°
540 nm	14.0	9.5	10.5	8.0	8.0	9.5	10.0	7.5	11.0	1.75
900 nm	14.5	11.0	12.0	10.0	10.0	11.0	11.0	8.0	12.0	2.25

passing through this film. The temperature at the crystal position was measured by a 0.003″ Pt and Pt-13 percent Rh thermocouple. The output of this thermocouple, read from a Keithley 160 Digital Multimeter, was calibrated to temperature by use of the melting points of anthracene (216°C), $NaNO_3$ (307°C), B_2O_3 (460°C), KIO_3 (560°C), $Ba(NO_3)_2$ (592°C), KCl (776°C), NaCl (801°C), and $BaCl_2$ (962°C). This was achieved by mounting these crystals on the quartz-glass capillaries and inserting them through the 1/8″ hole in the Macor furnace so they occupied the same site as the cylinder did later.

Photometric measurement of extinction positions

To measure extinction at the 540 nm wavelength, a 540 nm narrow-band-pass interference filter was inserted immediately below the objective. To measure extinction at the 900 nm wavelength, the Schott IR filter, set to pass 900 nm as the peak wavelength, was positioned above the ocular to intercept the light immediately prior to its entry into the photomultiplier tube. The IR filter was thus better positioned than the 540 nm filter to reduce the effect of stray light. The size of the 540 nm filter unfortunately prevented its insertion at this optimum site.

With the desired filter in place, a preliminary extinction position for the anorthite cylinder was determined by rotating the microscope stage until the response of the photomultiplier tube, as read from a Keithley 414A Picoammeter, reached a minimum. The refined extinction position was then determined by rotating the microscope stage slightly away from this preliminary position, first in one direction and then the opposite, stopping in each case when the picoammeter's needle reached the first scale division above its reading for the preliminary extinction position. These two microscope-stage positions, which between them bracket the preliminary extinction position, were then averaged to yield a refined extinction position. At least two refined extinction positions were determined for each spindle setting (S = 0°, 10° ···, 170°). In 90 percent of the cases, the two readings agreed so closely that more were not needed. For example, the average difference between the two refined positions for the eighteen spindle settings was, for wavelength 540 nm, 0.06° (*esd* = 0.07°) for measurements made at 500°C, and 0.08° (*esd* = 0.11°) for those at 850°C. For wavelength 900 nm, it was 0.09° (*esd* = 0.11°) at 500°C and 0.04 (*esd* = 0.06°) at 850°C.

Study of the Mijakejima anorthite, 25° to 850°C

For a cylinder of Mijakejima anorthite mounted on a Supper spindle stage, extinction measurements were made at wavelengths 540 and 900 nm at room temperature (while dry and while in an oil of n_D equal to 1.572) and also, while dry, at the temperatures 200°, 300°, 350°, 400°, 500°, 600°, 700°, 750°, 800°, and 850°C. Prior to measuring these latter extinctions, the crystal was held at each temperature for several hours (Table 5). Such extinction measurements were also made during cooling after the anorthite crystal had been held for about two hours[6] at 600°, 500°, 350°, 200°, and 25°C. Each set of extinction data was then solved by computer to determine $2V$ and the orientation of the two optic axes, the two bisectrices, and the optic normal for each temperature and wavelength.

Thermal variations in 2V and their interpretation

For wavelengths 540 and 900 nm, a plot of $2V_\alpha$ with increasing temperature (Fig. 6) shows a minimum near 350°C, a more precise evaluation awaiting a closer spacing of the temperatures of observation in this region. The continuous decrease in $2V_\alpha$ from 25° to (*ca.*) 350°C probably monitors the continuous and reversible transition first reported for anorthite by Brown *et al.* (1963). For an anorthite from the Vesuvius locality described by Kratzert (1921), these authors observed, in X-ray photographs taken at temperatures between 25° and 350°C, a gradual disappearance of the *c* reflections ($h + k$ even; l odd) as 350°C was approached, plus their reappearance upon cooling. In curves relating temperature to the extinction angle α':a for (001) cleavage flakes of the Kratzert anorthite, Bloss (1964) noted an inflection at about 341°C and suggested that it marked the temperature of disappearance of the *c* reflections.

For the Mijakejima anorthite, Foit and Peacor (1967) could not detect, in practice, the *c* reflections 025 and $0\bar{2}7$ above 285°C; however, their plots of their integrated intensities versus temperature, if ex-

[6] The full set of measurements was made at each temperature after a few of the more temperature-dependent extinction positions showed no measurable change after a one-hour lapse of time.

trapolated to zero intensity, yielded theoretical disappearances at 342° and 320°C. Later, Laves *et al.* (1970) noted the $06\bar{5}$ *c* reflection for anorthite to decrease in intensity so as to be practically nil at 400°C, with the most pronounced changes occurring at (*ca.*) 230°C. Consequently they concluded that this anorthite behaved predominantly as primitive anorthite below 230°C, but as body-centered anorthite above it. Smith (1974, p. 141) notes, "There is considerable unpublished discussion whether *c* diffractions retain intensity above 230°C, but the question is unresolved." Factors affecting the temperatures determined for disappearance of a *c* diffraction in anorthite likely include: (1) the original intensity at 25°C; (2) the sensitivity of the mode of detection; and (3) differences in composition and/or thermal history between specimens.

Although they provide no evidence as to the nature of the structural changes, changes of optical properties with temperature may equal or surpass X-ray methods in disclosing the temperatures at which such structural changes occur or achieve completion.

The plotted values of $2V_\alpha$ (Fig. 6) are systematically in error, because the crystal cylinder's extinction positions were measured in air so that the wave normal of the light was refracted away from the microscope's axis upon entering the crystal. Moreover, a truly cylindrical shape had not been achieved, the grinding and polishing having produced a slightly conical shape. Such errors from refraction were suppressed, if not eliminated, by immersing the cylinder in the 1.572 (n_D) oil. The systematic errors in the dry results are thus seen to be relatively small (Table 6). Moreover, all dry results for the same wavelength will likely incorporate the same systematic errors regardless of whether the cylinder's extinctions were measured at 25°, 200°, 300°C, *etc.* A comparison of the dry results for differing temperatures therefore seems valid.

Results I and II in Table 6 indicate that heating to 850°C followed by cooling to 25°C produced no permanent change (hysteresis) in either $2V_{540}$ or $2V_{900}$ as measured at 25°C. The heating and cooling cycle, however, may have caused the crystal itself to have moved slightly on the glass fiber, because the *S*, *E* coordinates change between I and II. For the slightly less accurate, dry results (III, IV, and V), again $2V$ at 25°C does not appear to have been changed significantly by heating to 850°C, then cooling. The *S*, *E* coordinates do change slightly for the "after cooling" results, probably in response to a slight shift in the crystal's position.

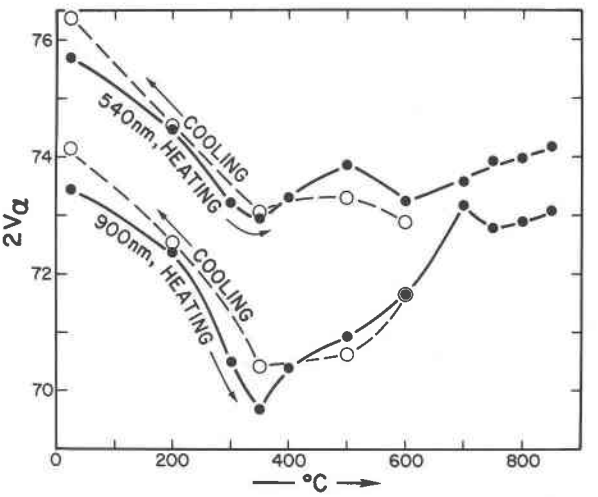

Fig. 6. Variation in $2V_\alpha$ for wavelengths 540 nm and 900 nm during heating (solid black dots) and during cooling (open circles) of the Mijakejima anorthite.

Temperature-induced positional changes

The temperature-induced positional changes of the five optic vectors proved relatively small, but fortunately the precision of the technique, even in air, seems excellent (*cf.* results IV and V, Table 6). As discussed, the crystal may have experienced a slight positional shift on the glass fiber. Many *but not all* of the plots showing the temperature-induced positional changes for each optic vector (Figs. 7 to 11) show irregularities between 400° and 700° during heating. These may indicate that the crystal moved slightly after 400°C but concluded its motion before 700°C. Despite this possibility of an experimental error that can easily be corrected, the results are exciting. They indicate the potential of such optical studies, at high (or low) temperatures, for determining the temperatures of phase transitions. Their detailed discussion now follows.

Thermal changes in optic axis A1. The optic axis here labeled *A1* changes position along a fairly regular course for wavelength 540 nm (Fig. 7A) from 25° up to 350° or 400°C. Its position at 500°C seems anomalous. From 600° to 850°C, its position changes little and experimental error may mask any trend. Cooled from 850° to 25°C, it failed to return to its original position for 25°C. For 900 nm, optic axis A1 changes regularly from 25° to 350°C (Fig. 7B), changes course abruptly from 350° to 600°C, and again from 700° to 850°C. The change in course begun at 350°C cannot be attributed to movement of the crystal on its mount because such movement would have produced a similar trend for 540 nm (Fig.

Table 6. Comparison of results at 25°C for the Mijakejima anorthite, before and after heat treatment, as determined from extinction measurements with the cylinder in oil and "dry." To save space, the estimated standard deviations, in terms of the least decimal cited, are here given as superscripts. Thus 78.0^3 represents a value of 78.0 with an *esd* of 0.3.

λ	2V	OA		OA		AB		OB		ON	
		S	E	S	E	S	E	S	E	S	E
I. At 25°C, in 1.572 oil, before heating											
540	78.0^3	101.7^2	64.0^2	170.2^2	104.6^1	137.4^2	83.1^1	42.8^1	56.7^2	57.7^3	145.8^2
900	76.4^2	102.4^2	64.5^1	169.7^2	103.9^1	137.4^2	83.0^1	42.9^1	57.2^1	58.0^3	146.3^2
II. At 25°, in 1.572 oil, after cooling from 850°C											
540	78.1^1	103.8^1	61.9^1	170.5^1	105.9^1	138.8^1	82.7^1	43.4^1	53.8^1	58.5^1	142.8^1
900	76.6^1	104.8^1	62.3^1	170.3^1	105.2^1	139.1^1	82.6^1	43.7^1	54.1^1	59.2^1	143.1^1
III. At 25°, in air, before heating											
540	75.7^4	103.0^3	63.1^2	168.8^3	103.9^2	137.5^2	82.2^1	42.1^2	55.6^2	58.5^4	144.5^2
900	73.5^4	106.3^3	63.2^2	170.2^3	102.7^2	139.8^2	81.7^1	44.2^2	55.9^2	61.6^4	144.6^2
IV. At 25°, in air, soon after cooling from 850°C											
540	75.8^2	105.4^2	61.7^1	169.7^2	105.2^1	139.2^1	82.3^1	43.4^1	53.3^1	59.2^2	142.2^1
900	74.3^5	106.9^3	62.2^3	170.3^3	104.1^3	140.2^3	82.0^2	44.3^2	54.1^3	61.0^5	142.9^3
V. At 25°C, in air, 7 days after cooling from 850°C											
540	76.4^2	105.4^2	61.8^1	170.2^1	105.4^1	139.5^1	82.4^1	43.8^1	53.3^1	59.4^2	142.3^1
900	74.2^5	106.9^3	62.3^3	170.3^3	104.1^2	140.2^3	82.0^2	44.4^2	54.1^3	61.0^5	143.0^3

7A). Upon cooling, A1 returned to its former position at 600°C, then to a somewhat anomalous position at 500°C (experimental error?), and from 350° to 25°C followed a course roughly parallel to the heating curve, but it did not return to its pre-heating position at 25°C.

Thermal changes in optic axis A2. For wavelength 540 nm, the position of the optic axis here called *A2* did not change position nearly as much from 25° to 400°C as had A1 (*cf.* Figs. 8A and 7A). Its positions at 500° and 600°C were disparate but from 700° to 850°C a regular course was reestablished. With cooling from 600° to 25°C, the course of A2 somewhat resembles its heating curve from 25° to 400°C, except for the reversal in direction from 200° to 25°C. Again this position at 25°C differs from its pre-heating position at 25°C. For wavelength 900 nm, the heating curve for A2 (Fig. 8B) would have been regular except for the anomalous positions at 300°, 350°, and 700°C. These may represent experimental errors. Indeed the least-squares residual after the solution of the 350°C data was very large (0.00675); however, that for 300°C was not (0.00094).

Reinhard's (1931) classic stereogram shows how, relative to the crystallographic axes, the two optic axes of plagioclase change position as composition varies from An_0 to An_{100}. In response to such compositional change, one optic axis, (symbolized *B* by Reinhard) changes position markedly whereas the other (symbolized *A*) does not, its positional change with composition appropriately describing an inverted question mark. Interestingly, X-ray studies of the anorthite cylinder disclosed that the optic axis here designated *A2* corresponds to the compositionally "active" optic axis symbolized *B* by Reinhard.

Thermal variations in positions of AB, OB, and ON. With increasing temperature the acute bisectrix (AB) for wavelength 540 nm follows a fairly regular path

(Fig. 9A) from 25° to 800°C, except at 500° and 600°C. The cooling curve (dashed) is also quite regular between 500° and 25°C. For 900 nm (Fig. 9B), the cooling and heating curves are fairly regular except for the 300°C heating value which, for 900 nm, appears to incorporate considerable experimental error.

The obtuse bisectrix for 540 nm follows a regular course (Fig. 10A) when heated from 25° to 400°C and from 600° to 850°C. The 500°C value seems off. The cooling curve from 600° to 25°C seems quite regular. For 900 nm, the obtuse bisectrix (Fig. 10B) follows one course from 25° to 350°, then another course to 700°C. Its cooling curve is fairly regular from 600° to 25°C. The optic normal for 540 nm (Fig. 11A) follows along the same trend from 200° to 400°C, but the points at 500° and 600°C fluctuate widely from this trend. From 700° to 850°C, a fairly regular trend has been reestablished. The cooling curve (dashed) is fairly regular except for the transposal of the values for 500 and 600°C. The heating

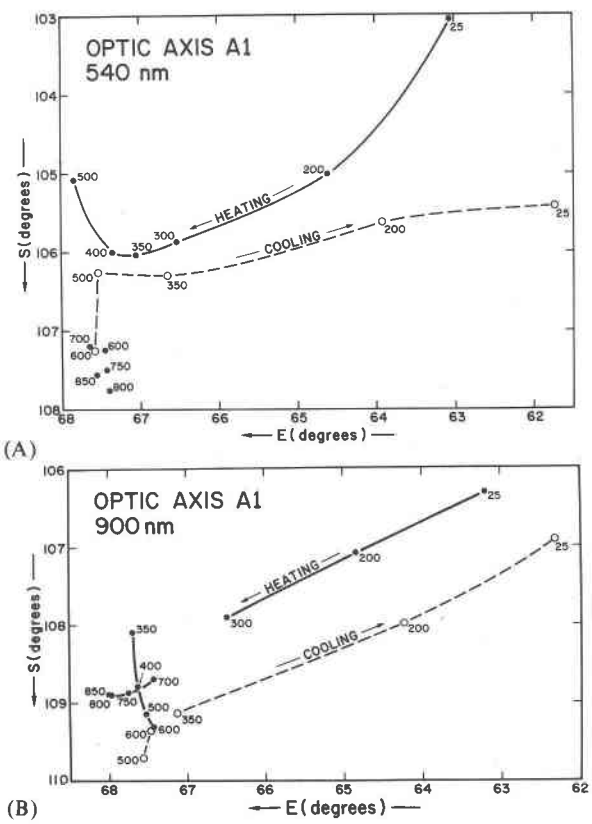

Fig. 7. Positional variation with temperature of the optic axis A1 of the Mijakejima anorthite during heating (solid circles) and cooling (open circles) for wavelengths (A) 540 nm and (B) 900 nm. The S and E coordinates are stereographic spindle-stage coordinates as defined by Bloss and Riess (1973).

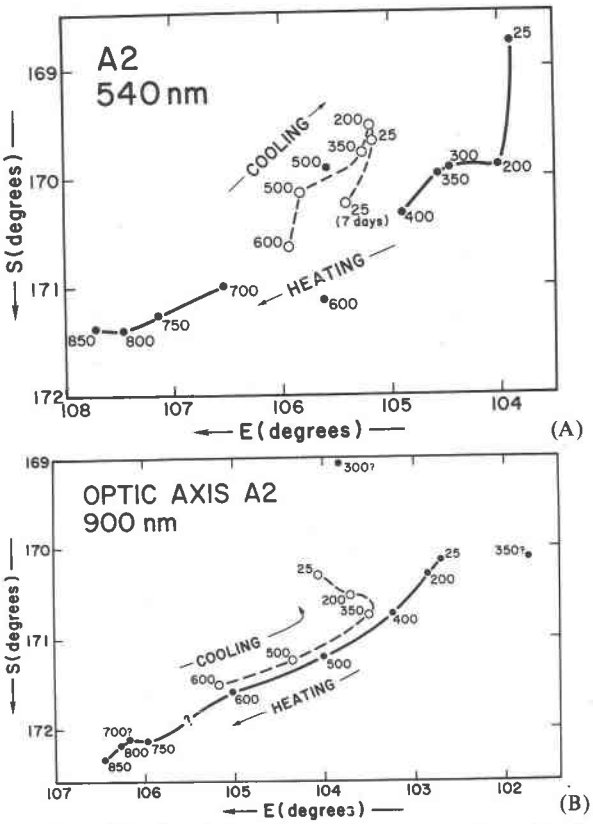

Fig. 8. Positional variation with temperature of the optic axis A2 for the Mijakejima anorthite during heating (solid circles) and cooling (open circles) for wavelengths (A) 540 nm and (B) 900 nm.

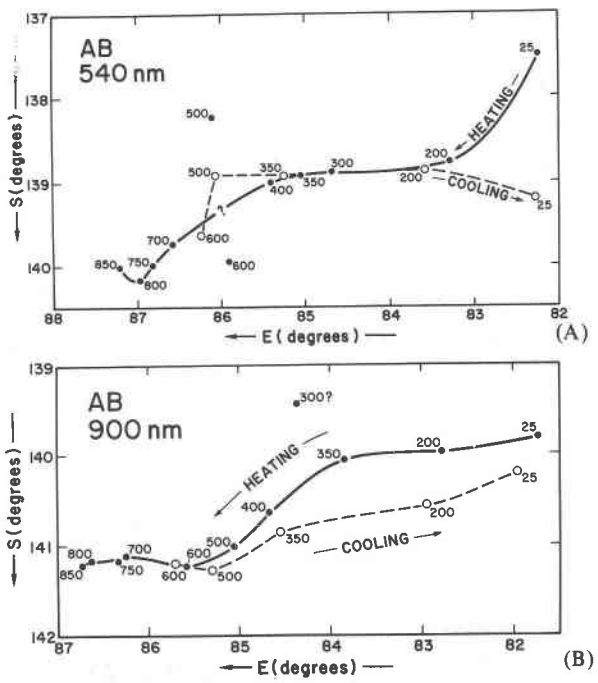

Fig. 9. Positional variation with temperature of the acute bisectrix for wavelengths (A) 540 nm and (B) 900 nm.

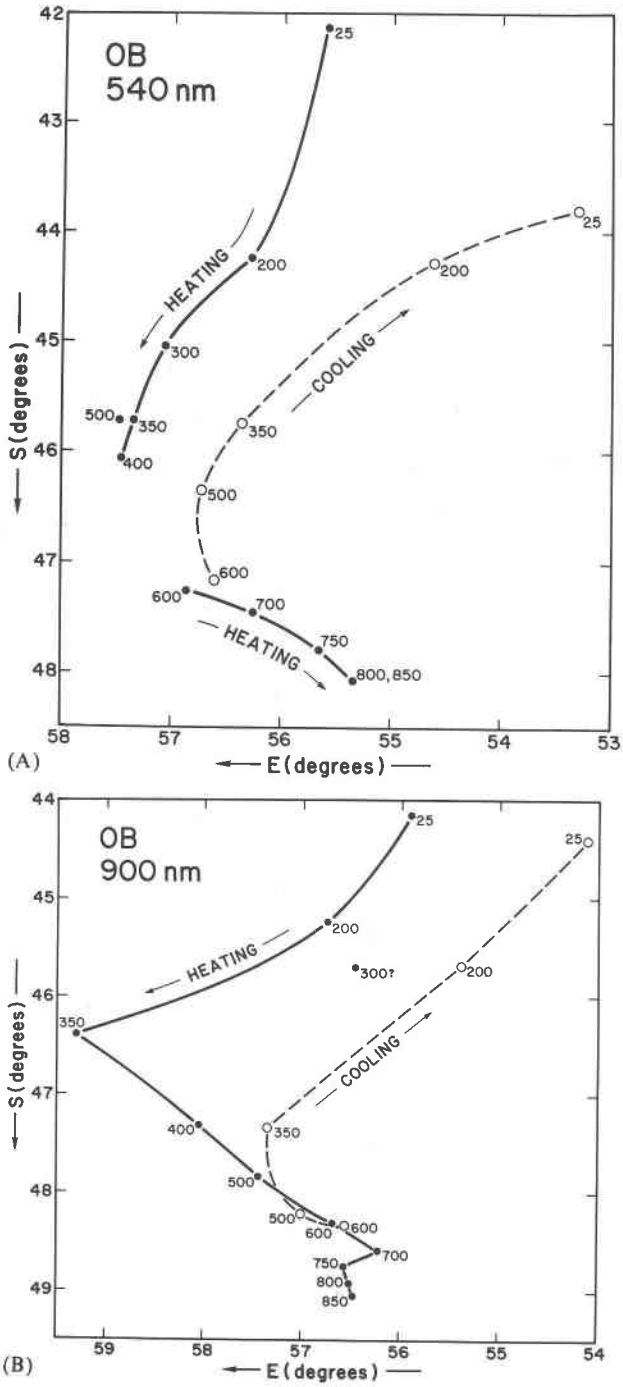

Fig. 10. Positional variation with temperature of the obtuse bisectrix for wavelengths (A) 540 nm and (B) 900 nm.

curve for the optic normal for 900 nm (Fig. 11B) displays an abrupt change in course at 350°C. This is also true for the cooling curve.

Conclusions

1. The Bloss-Riess technique performed at elevated (or sub-zero) temperatures will, in many cases, permit determination of the temperatures at which subtle phase transitions begin (or achieve completion).

2. Such optical studies will greatly augment X-ray studies, since light wavelengths, being longer than X-ray's, may average over a larger domain and thus provide a different information content.

3. The dispersion of the five significant vectors for biaxial crystals—namely, the two optic axes, the two

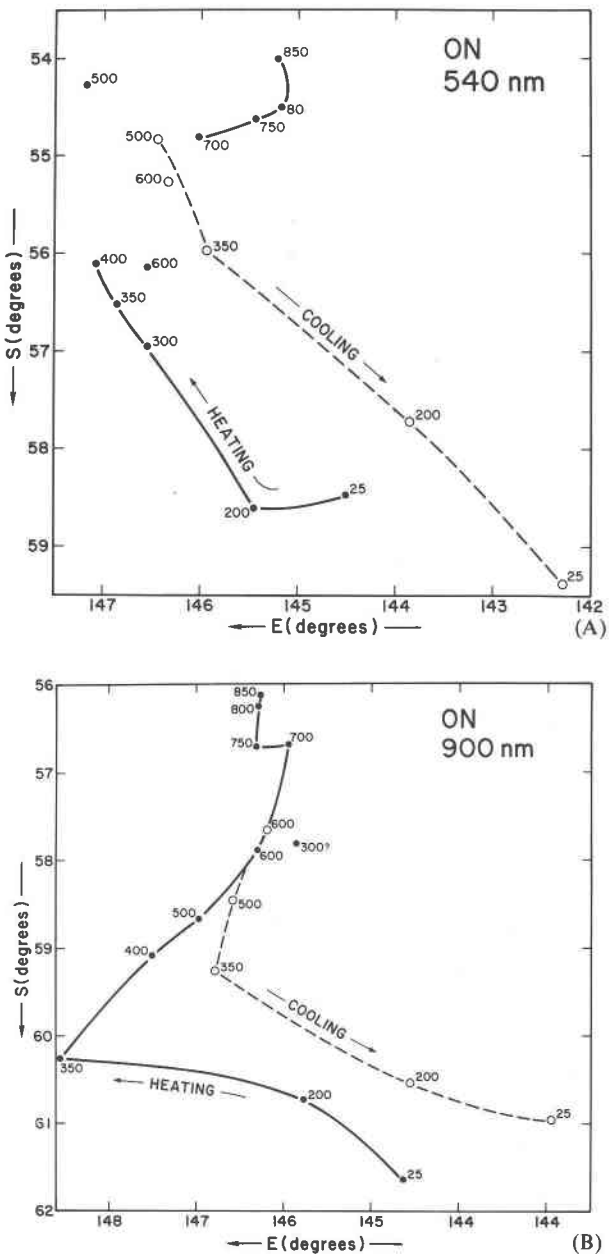

Fig. 11. Positional variation with temperature of the optic normal for wavelengths (A) 540 nm and (B) 900 nm.

bisectrices, and the optic normal—can now be assessed quantitatively from extinction measurements made at two widely different wavelengths.

4. Photometric measurements of extinction permit the value of $2V$ and the orientation of the indicatrix to be determined for wavelengths beyond the visible.

5. The spindle stage, used in conjunction with the dispersion or double-variation method and with Equation 1 to smooth the data, permits refractive indices (and their dispersion) to be measured with greater routine accuracy than heretofore.

6. The entire optical data base for transparent crystals needs to be verified, expanded, and upgraded through a more universal use of spindle-stage techniques.

Acknowledgments

I am indebted to the Earth Sciences Section of the National Science Foundation for financial support under grant GA-32444 during the early developmental stages (1972–1974) of these optical techniques and programs. Virginia Polytechnic Institute and State University kindly provided computing funds at all times, as well as partial support of this research after termination of grant GA-32444. My colleagues Professors G. V. Gibbs, P. H. Ribbe, D. R. Wones, and I. J. Good helped in many ways. For aid in developing the forerunning Bloss-Riess program I thank Drs. S. J. Louisnathan, M. G. Bown, R. D. Riess, and Mr. Ed Wolfe. For recent reorganization of this program and addition to it of DISPER, I thank Mr. Michael Rohrer, who proved a tower of strength. The high-temperature extinction measurements on anorthite were performed almost entirely by my assistant, Kevin Selkregg, and I thank him for his careful work and for his great enthusiasm toward these new optical methods. I regret that time prevented discussion of the optical properties of the very interesting orthopyroxene crystals kindly sent me by Professor Subrata Ghose of the University of Washington. I am indeed grateful to him for supplying them.

Last but not least, I wish to thank Dr. Ray E. Wilcox of the U. S. Geological Survey, whose repeated urgings ultimately succeeded in getting me to try spindle-stage methods. Since single-axis stages had been in use over 100 years ago and, indeed, had evolved into the multi-axial U-stage, to revert to one seemed like it might be a backward step. Not so! For single crystals, the power and simplicity of single-axis methods convert almost any polarizing microscope into a versatile device for routine and research measurements of optical constants. Among amateur mineralogists, so-called because they study minerals for sheer joy and earn their livelihood elsewhere, Dr. Curt Segeler and Mr. Ross Anderson have shown a bubbling enthusiasm in using the spindle stage to identify minerals in their home laboratories, and in converting even professional mineralogists to the techniques.

References

Bloss, F. D. (in press) *The Spindle Stage: Principles and Practice.* Geopress, P. O. Box 662, Blacksburg, Virginia 24060.

——— (1964) Optical extinction of anorthite at high temperatures. *Am. Mineral., 49,* 1125–1131.

——— and J. F. Light (1973) The detent spindle stage. *Am. J. Sci., 273-A,* 536–538.

——— and S. J. Louisnathan (1974) Accurate routine measurement of refractive indices (abstr.). *Geol. Soc. Am. Abstr. with Programs, 6,* 659.

——— and D. Riess (1973) Computer determination of $2V$ and indicatrix orientation from extinction data. *Am. Mineral., 58,* 1052–1061.

Brown, G. E., S. Sueno and C. T. Prewitt (1973) A new single-crystal heater for the precession camera and four-circle diffractometer. *Am. Mineral., 58,* 698–704.

Brown, W. L., W. Hoffmann and F. Laves (1963) Über kontinuierliche und reversible Transformation des Anorthits ($CaAl_2Si_2O_8$) zwischen 25 und 350°C. *Naturwissenschaften, 50,* 221.

Emmons, R. C. (1928) The double dispersion method of mineral determination. *Am. Mineral., 13,* 504–515.

Foit, F. F. and D. R. Peacor (1967) High temperature diffraction data on selected reflections of an andesine and anorthite. *Z. Kristallogr., 125,* 1–6.

Good, I. J. (1958) Significance tests in parallel and in series. *J. Am. Stat. Assn., 53,* 799–813.

Jenkins, F. A. and H. E. White (1976) *Fundamentals of Optics.* McGraw-Hill, New York.

Jones, F. T. (1968) Spindle stage with easily changed liquid and improved crystal holder. *Am. Mineral., 53,* 1399–1403.

Kolb, R. (1911) Verleich von Anhydrit, Cölestin, Baryt, und Anglesite in bezug auf die Veränderung ihrer geometrischen und optischen Verhältnisse mit der Temperatur. *Z. Kristallogr., 49,* 14–61.

Kratzert, J. (1921) Die kristallographischen und optischen Konstanten des Anorthits vom Vesuv. *Z. Kristallogr., 56,* 465.

Laves, F., M. Czank and H. Schulz (1970) The temperature dependence of the reflection intensities of anorthite ($CaAl_2Si_2O_8$) and the corresponding formation of domains. *Schweiz. Mineral. Petrogr. Mitt., 50,* 519–525.

Leisen, E. (1934) Beitrag zur Kenntnis der Dispersion der Kalknatron-feldspäte. *Z. Kristallogr., 89,* 49–79.

Louisnathan, S. J., F. D. Bloss and E. J. Korda (1978) Measurement of refractive indices and their dispersion. *Am. Mineral., 63,* 394–400.

Mandarino, J. A. (1977) Old mineralogical techniques. *Can. Mineral., 15,* 1–2.

Merwin, H. E. and E. S. Larsen (1912) Mixtures of amorphous sulfur and selenium as immersion media for the determination of high refractive indices with the microscope. *Am. J. Sci., 34,* 42–47.

Reinhard, M. (1931) *Universal Drehtischmethoden.* Wepf, Basel, Switzerland.

Roberts, M. J. T. (1975) Indicatrix orientation for barium feldspars referred to crystallographic axes using X-ray and extinction data. *Am. Mineral., 60,* 1113–1117.

Smith, J. V. (1974) *Feldspar Minerals,* v. 1. Springer-Verlag, New York.

Wilcox, R. E. (1959) Use of the spindle stage for determining refractive indices of crystal fragments. *Am. Mineral., 44,* 1272–1293.

Winchell, A. N. and H. Winchell (1951) *Elements of Optical Mineralogy, Pt. II: Descriptions of Minerals.* Wiley, New York.

Wright, H. G. (1966) Determination of indicatrix orientation and $2V$ with the spindle stage: a caution and a test. *Am. Mineral., 51,* 919–924.

Manuscript received, January 28, 1978; accepted for publication, January 28, 1978.